shifts and/or intensity alterations (Figure 6b and Table VI).

In C_s symmetry all 12 fundamental vibrational modes of S_4N_2 are expected to be infrared active, but in C_{2v} (planar) symmetry one vibration (an out-of-plane ring deformation A_2) will become inactive. It is therefore interesting to speculate whether the disappearance of the 561-cm^{-1} band in liquid and dissolved samples represents a net increase in symmetry of S_4N_2. However, isotopic substitution with ^{15}N indicates virtually no isotope shift for the 561- and 469-cm^{-1} bands, suggesting that they are the ν_{asym} and ν_{sym} modes of the S-S-S group. In H_2S_3 these vibrations are observed at 477 and 487 cm^{-1}.[42] Thus, if the 561-cm^{-1} band is the ν_{asym}(S-S-S) stretching mode, its disappearance on phase change is hard to explain, since, regardless of any symmetry change, it should remain infrared active. The resolution of the problem is beyond the scope of the present study. As Table VI indicates, the number of vibrations which undergo isotope shifts indicates that S_4N_2 is a strongly coupled system and not amenable to an elementary vibrational analysis.

Summary

The X-ray crystal structure determination of S_4N_2 has established that the molecule is a nonplanar ring, with the central sulfur of the trisulfide sequence lifted out of the plane of the remaining five atoms. The calculated barrier for the half-chair/half-chair inversion is approximately 6-10 kcal mol^{-1}. On the basis of ab initio HFS molecular orbital calculations, the electronic structure of planar S_4N_2 can be satisfactorily rationalized in terms of interacting S_3 and NSN fragments. Although there is significant *net* π bonding in the NSN moiety, there is essentially no *net* π bonding for the remaining N-S and S-S links. In the half-chair conformation the σ system in the S_3 and NSN fragments is strengthened at the expense of weakened central N-S bonds, the net effect favoring the nonplanar geometry. The electronic spectrum of S_4N_2 exhibits two strong low-energy transitions which we assign to HOMO (π^*-type) → LUMO (π^*-type), and HOMO - 1 (π^*-type) → LUMO (π^*-type) transitions.

Acknowledgment. We thank the Natural Sciences and Engineering Research Council of Canada and FINEP of Brazil for financial support and for an NSERC University Research Fellowship (to R.T.O.). We are grateful to Kim Wagstaff for his assistance in obtaining the MNDO and HFS results.

Registry No. S_4N_2, 32607-15-1; S_2Cl_2, 10025-67-9; NH_4OH, 1336-21-6; ^{15}N, 14390-96-6.

Supplementary Material Available: A listing of structure factor amplitudes and a table of anisotropic thermal parameters for S_4N_2 (3 pages). Ordering information is given on any masthead page.

Crystal Structure of Dehydrated Ca-Exchanged Zeolite A. Absence of Near-Zero-Coordinate Ca^{2+}. Presence of Al Complex

Joseph J. Pluth and Joseph V. Smith*

Contribution from the Department of the Geophysical Sciences, The University of Chicago, Chicago, Illinois 60637. *Received April 19, 1982*

Abstract: After various exchange procedures were tested, crystals of Linde zeolite 4A were exchanged with 1 M $CaCl_2$ solution at room temperature for 6 days. Electron microprobe analysis gave $Na_{0.4}Ca_{5.2}Al_{11.5}Si_{12.5}O_{48}\cdot xH_2O$ with a possible trace of K and Mg. X-ray diffraction data for a crystal dehydrated at 350 °C were refined in space group $Fm\bar{3}c$ (a = 24.44 Å). Because of weakness of diffraction intensities, the mean T-O distances (1.58 and 1.73 Å) have low precision but are consistent with the earlier evidence for alternation of tetrahedra populated by Si and $\sim Al_{0.9}Si_{0.1}$. All Ca atoms lie near the center of 6-rings, and the electron density found in an 8-ring by earlier investigators is attributed to potassium scavenged during ion exchange. Approximately four-fifths of the Ca atoms (4.4 atoms per pseudocell) project into the large cage, and one-fifth (1.2 atoms) project into the sodalite unit. Both are bonded to three O(3) at about 2.3 Å. Electron density in the sodalite unit is attributed to Al in a tetrahedron of oxygen species, disordered into two orientations. All data are consistent with a cell content near $Ca_{5.3}Na_{0.4}Al_{11.0}Si_{13.0}O_{48}\cdot(Al_{0.3}O_{0.6}H_{0.3})$ in which the suggested H content is completely speculative.

A new determination of the crystal structure of dehydrated Sr-exchanged zeolite A[1] revealed Sr atoms only at the 6-rings and led to the suggestion that electron density found near the 8-rings in an earlier determination[2] actually resulted from introduction of potassium during ion exchange with impure solution. The present structure determination of dehydrated Ca-exchanged A provides a further test of this alternate interpretation to the now suspect claim of near-zero-coordination for divalent cations.[2,3] It also provides further evidence for an occluded tetrahedral complex produced during ion exchange with a divalent ion.

Experimental Section

Specimen Preparation. Crystals of zeolite 4A (Na-A) were prepared by a modification of Charnell's method[4] including a second crystallization using seed crystals from the first synthesis. Ion exchange at 95° C for 5 days with 1 M $CaCl_2$ solution (Alfa Optronic Grade 87607) resulted in occlusion of a chlorine species detected by electron microprobe analysis. Exchange at room temperature for 6 days, followed by thorough washing with deionized water, obviated occlusion of chlorine, but the crystals contained residual sodium. Exchange at room temperature for 2 weeks with two changes of water saturated with $Ca(OH)_2$ (Baker Analyzed Reagent 1372) yielded crystals of composition near $Na_{1.4}K_{0.7}Mg_{0.2}Ca_{4.6}Al_{11.6}Si_{12.4}O_{48}\cdot xH_2O$, and it was concluded that a trace of K, and perhaps Mg (but analyses near detection level), had been scavenged from the saturated solution which contains only 0.17 wt.% $Ca(OH)_2$ at 25 °C. Atomic absorption analysis of the saturated solution revealed the following weight ratios of Ca/Na/K/Mg: 97.9/1.7/0.4/<0.0002. Samples exchanged with 0.5 M solution of $Ca(ClO_4)_2$ (Alfa 22112) and an equal-volume mixture of 0.5 M $Ca(ClO_4)_2$ and saturated $Ca(OH)_2$ showed residual Na (~0.4 atom/48 oxygen) even after exchange for 2 months.

Crystals with properties given in ref 5 and 6 were selected for X-ray and electron microprobe measurements from the batch exchanged with

(1) Pluth, J. J.; Smith, J. V. *J. Am. Chem. Soc.* **1982**, *104*, 6977-6982.
(2) Firor, R. L.; Seff, K. *J. Am. Chem. Soc.* **1978**, *100*, 3091-3096.
(3) Firor, R. L., Seff, K. *J. Am. Chem. Soc.* **1978**, *100*, 978-980.
(4) Charnell, J. F. *J. Cryst. Growth* **1971**, *8*, 291-294.
(5) Pluth, J. J.; Smith, J. V. *J. Phys. Chem.* **1979**, *83*, 751-759.
(6) Pluth, J. J.; Smith, J. V. *J. Am. Chem. Soc.* **1980**, *102*, 4704-4708.

0002-7863/83/1505-1192$01.50/0

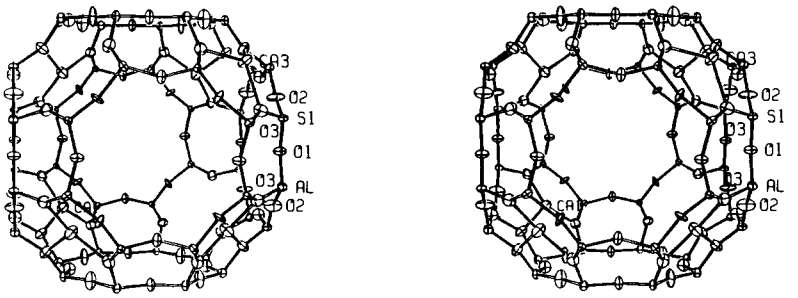

Figure 1. Stereoplot of large cage with representative positions for Ca atoms Ellipsoids at 30% probability level.

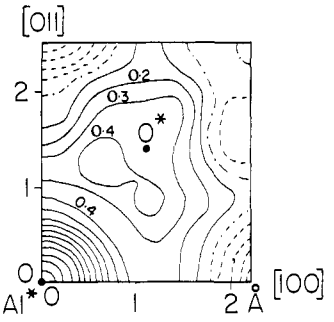

Figure 2. Residual electron density in (110) plane passing through the origin. Zero and negative contours, dot-dash and dash, respectively. Contours at 0.1 e/Å^3 up to 0.4 and then at 0.4 up to 4.0 e/Å^3.

1 M $CaCl_2$ solution at room temperature. The mean and 1σ spreads for 26 analyses following the procedure in ref 5 gave the following numbers of atoms calculated to 48 oxygens: Na 0.42 (0.32), Mg 0.14 (0.13), Al 11.57 (0.14), Si 12.59 (0.11), K 0.07 (0.06), Ca 5.15 (0.23). It should be emphasized that the amounts of Mg and K are close to the detection level when account is taken of possible systematic errors, and the following rounded-off composition will be used: $Na_{0.4}Ca_{5.2}Al_{11.5}Si_{12.5}O_{48}$. The Al and Si analyses confirm the earlier evidence[1,5,6] for an Al/Si ratio less than unity. The analyses of the exchangeable cations are too low for charge balance even when K and Mg are added (11.07 charges vs. 11.5 Al), and the possibility of some unanalyzed H-bearing species must be considered (see later).

A cube (sample PS) was lodged in a silica capillary and dehydrated under 10^{-5} torr at 350 °C for 1 day. After the sample was sealed under vacuum at temperature, it was cooled slowly to room temperature.

X-ray Data Collection. The conditions for data collection (Table I) are similar to those for dSr-A[1] and are compared with those used by Firor and Seff (FS).[2] All crystals of Ca-exchanged A decomposed after storage for 1 year after X-ray data collection, and the weakness of the intensities collected for crystal PS probably result from partial decomposition as indicated by variable opacity in an optical microscope. All PS diffractions obey $Fm\bar{3}c$ at the 2σ detection level, but the observed intensity of 83 ± 42 for the 111 diffraction may be in violation (cf. dSr-A).[1] Only 25 significant intensities refer to the 24-Å superstructure, and the structure refinement is based mainly on the 311 significant intensities for the pseudostructure.

Structure Refinement. Least-squares refinements (labeled f) of the PS data set converged rapidly for the 24-Å supercell in $Fm\bar{3}c$ in spite of correlation coefficients up to 0.9 and the small number of pseudostructure intensities. Starting parameters for framework atoms were taken from dNa-A,[6] and two sites were used for Ca, displaced into either the supercage Ca(1) or the sodalite unit Ca(3) from the center of the 6-ring (Figure 1). There was no significant electron density near the plane of the 8-ring, and site Ca(4) from ref 2 was ignored. However, just as for dSr-A,[1] residual electron density was found at the center of the sodalite unit (sharp spherical peak 4.4 e/Å^3; coordinates 0,0,0) and at eight symmetry-related positions on the body diagonals (irregular peak near ±0.04, ±0.04, ±0.04). The (110) planar section (Figure 2) is similar to those for two crystals of dSr-A[1] when account is taken of experimental error, and the electron density was modeled by two AlO_4 tetrahedra, each of which accounts for half of the origin peak and four out of the eight irregular peaks (Figure 3). Averaging of the two tetrahedral orientations generates the cubic array of eight peaks around the origin peak. Inclusion of the Al* position at the origin in the least-squares refinement caused the conventional R and R_w indices to fall from 0.065 and 0.060 to 0.055 and 0.045. Further reduction to 0.046 and 0.035 resulted from addition of O* fixed at 1.74 Å from Al*. Refinement in the pseudocell (p) provided a comparison (Table II) with the refinement by Firor and Seff (FSp).[2]

The least-squares refinements used atomic scattering factors and anomalous scattering corrections for Si^{2+}, Al^+, O^-, and Ca^{2+} from "International Tables for X-ray Crystallography", with interpolation

Table I. X-ray Diffraction Data and Structure Refinement

	PSp,f	FSp
exchange soln, T	1 M $CaCl_2$, 25 °C	0.025 M $Ca(OH)_2$, 25 °C
dehydration temp, °C	350 °C	350 °C
cryst diameter, μm	84	80
space group	$Fm\bar{3}c$	$Pm\bar{3}m$
wavelength, Å	1.5418	0.710 69
monochromator	graphite	graphite
cell dimensions, Å	24.443 (2)	12.278 (2)
diffractometer	Picker FACS-1	Syntex $P\bar{1}$
orientation	~8° from a	?
scan technique	fixed θ–2θ	θ–2θ
speed, deg min^{-1}	2	1
range, deg	2.4–4.3	~1.6
background	fixed 40 s	variable, scan/bkgd = 1
total intensities measd	3324 (1809)[a]	~1700
unique data set	580 (369)[a]	884
significant data set	311 (286)[a] 2σ	303 3σ
(sin θ)/λ max	0.59	0.81
absorption coeff, cm^{-1}	78.7	~8.2
absorption correctn	yes	no
R	0.046 (0.042)[a]	0.084
weighted R	0.035 (0.034)[a]	0.066
S	1.9 (1.9)	3.1

[a] Numbers in parentheses refer to pseudostructure.

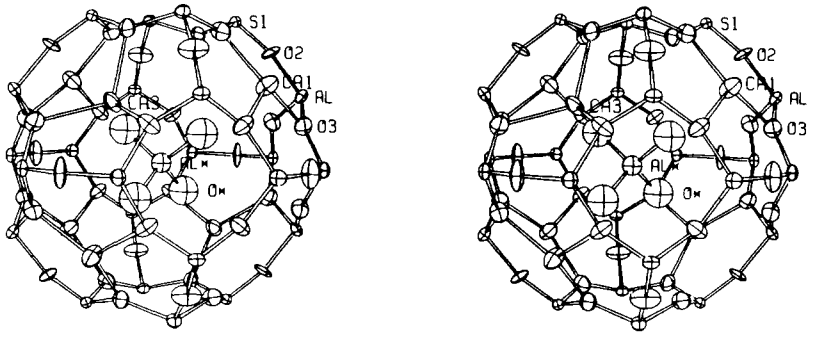

Figure 3. Stereoplot of sodalite unit and one of the AlO_4* tetrahedral units. Invert through the center to obtain the second orientation.

Table II. Atomic Populations, Positions, and Displacements of Dehydrated Ca-Exchanged Zeolite A[a]

	PSf			
	Si	Al	PSp	FSp
T				
position	96 (i)	96 (i)	24 (k)	24 (k)
population	96	96	24	24
x	0	0	0	0
y	0.0927 (3)	0.1869 (3)	0.1827 (1)	0.1828 (3)
z	0.1838 (2)	0.0899 (4)	0.3705 (1)	0.3715 (2)
β_{11}	13.3 (1.4)	11.6 (1.5)	49 (1)	40 (3)
β_{22}	7.3 (1.2)	8.8 (1.4)	37 (1)	22 (2)
β_{33}	6.5 (1.1)	10.9 (1.6)	32 (1)	17 (2)
β_{12}, β_{13}	0	0	0	0
β_{23}	0.3 (0.9)	3.3 (1.0)	5 (1)	2 (2)
Ca(1)				
position	64 (g)		8 (g)	8 (g)
population	34.8 (1.3)		4.4 (2)	3
x, y, z	0.1029 (4)		0.2057 (9)	0.2113 (10)
$\beta_{11}, \beta_{22}, \beta_{33}$	21.1 (1.1)		85 (4)	67 (9)
$\beta_{12}, \beta_{13}, \beta_{23}$	6.5 (1.2)		26 (5)	34 (10)
Ca(2)				
position				8 (g)
population				1
x, y, z				0.1908 (21)
$\beta_{11}, \beta_{22}, \beta_{33}$				
$\beta_{12}, \beta_{13}, \beta_{23}$				
B				0.3 (6)
Ca(3)				
position	64 (g)		8 (g)	8 (g)
population	9.8 (1.4)		1.2 (2)	1
x, y, z	0.0786 (14)		0.1571 (30)	0.1578 (15)
$\beta_{11}, \beta_{22}, \beta_{33}$	18 (4)		70 (17)	
$\beta_{12}, \beta_{13}, \beta_{23}$	8 (4)		32 (15)	
B				1.4 (6)
Ca(4)				
position				12 (i)
population				1
x				0
y, z				0.4683 (35)
β_{11}				1376 (329)
β_{22}, β_{33}				91 (52)
β_{12}, β_{13}				0
β_{23}				18 (49)

	PSf	PSp	FSp
O(1)			
position	96 (i)	12 (h)	12 (h)
population	96	12	12
x	0	0	0
y	0.1076 (3)	0.2153 (5)	0.2190 (8)
z	0.2469 (10)	0.5	0.5
β_{11}	22.2 (1.4)	88 (5)	75 (11)
β_{22}	20.7 (1.3)	82 (5)	54 (9)
β_{33}	7.9 (1.6)	40 (4)	25 (8)
β_{12}, β_{13}	0	0	0
β_{23}	1 (3)	0	0
O(2)			
position	96 (i)	12 (i)	12 (i)
population	96	12	12
x	0	0	0
y	0.1422 (8)	0.2885 (3)	0.2882 (6)
z	0.1461 (8)	y	y
β_{11}	45 (2)	182 (8)	148 (15)
β_{22}	17 (4)	53 (3)	35 (5)
β_{33}	8 (3)	β_{22}	β_{22}
β_{12}, β_{13}	0	0	0
β_{23}	8.4 (1.2)	31 (4)	21 (8)
O(3)			
position	192 (j)	24 (m)	24 (m)
population	192	24	24
x	0.0535 (6)	0.1116 (2)	0.1116 (4)
y	0.0581 (6)	x	x
z	0.1677 (2)	0.3354 (3)	0.3383 (5)
β_{11}	20 (3)	77 (2)	43 (4)
β_{22}	16 (2)	β_{11}	β_{11}
β_{33}	18 (1)	71 (3)	53 (6)
β_{12}	8 (1)	26 (3)	22 (10)
β_{13}	−2 (2)	−8 (2)	2 (4)
β_{23}	−2 (2)	β_{13}	β_{13}
Al*			
position	8 (b)	1 (a)	
population	2.4 (2)	0.30 (3)	
x, y, z	0	0	
B	5.4 (1.2)	5.3 (1.1)	
O*			
position	64 (g)	8 (g)	
population	9.6	1.2	
x, y, z	0.0411	0.0822	
B	13.1 (2.5)	13.2 (2.5)	

[a] Estimated standard deviations given in parentheses to the same significance level as parameters. x, y, z given as decimal fraction of cell edge. Isotropic B given in Å^2. Anisotropic displacement factor given as $10^4 \exp[-\Sigma\Sigma\beta_{ij}h_ih_j]$.

between factors for Si and Si^{3+} and for Al and Al^{3+}. The refinement in $Pm\bar{3}m$ used $(Si^{2+} + Al^{+})/2$. The largest positive peak (0.4 e/Å^3) in the final difference Fourier map at $0,0,^1/_4$ is approximately equal to the largest negative peaks.

Discussion

Framework. The mean distances for the two types of tetrahedra (1.58 and 1.73 Å) are consistent with the earlier conclusion that Si and Al atoms show strong alternation on the tetrahedral sites of zeolite A (e.g., ref 1) but are not accurate enough to provide estimates of fractional occupancy.

It is sufficient to consider the framework geometry of just the pseudocell. Significant differences between the PSp and FSp coordinates are consistent with presence of some potassium in the FS specimen. All T–O–T and O–T–O angles in the FSp data set are within experimental error of a linear model between PSp refinements of dCa-A and dK-A (Table III). The biggest difference of 3.4 ± 1.2° for the T–O(1)–T angle would correspond to replacement of about one-seventh of the Ca by 2 K. A slight complication arises from the residual Na in the PS crystal of Ca-exchanged A and from the presence of the AlO_4* complex, but the effects are probably less than those of the suggested K substitution in the FS crystal of dCa-A.

The O–T–O angles for dCa-A are almost the same as those for dSr-A (Table III), as expected because of the closely similar distribution of cation charges. However, the T–O–T angles differ by 10°, 11°, and 6°, probably in response to "twisting" of the framework caused by movement of O(3) away from the center of the cube of T atoms as the Sr–O(3) distances of ~2.4 Å are reduced to the Ca–O(3) distances of ~2.3 Å. Model calculations will be presented in a separate paper.

Calcium Positions. The present refinement for an analyzed crystal shows Ca positions only near to the 6-rings and not near to the 8-rings. It is suggested that position Ca(4) in ref 2 is actually occupied by K because (a) the framework geometry is consistent with this suggestion (preceding section), (b) the coordinates for position Ca(4) are consistent within experimental error with those for position K(2) in dK-A,[5] and (c) scavenging of K from impure Ca-bearing solution might be more intense for the flow technique used in ref 2 than for the constant-volume technique used here. Position Ca(4) of ref 2 was confirmed by calculation of a difference Fourier map for FS data. For this new interpretation of position Ca(4), the distances of 3.08 (4) and 3.13 (6) Å to O(1) and O(2) are not unusual when account is taken of incorrect distances produced by averaging with oxygen positions not bonded to an atom in position Ca(4), and the concept of

Table III. Interatomic Distances (Å) and Angles (deg) of Dehydrated Ca-Exchanged Zeolite A and Related Structures

	PSt						
	Si	Al	PSp	FSp	dK-A[5]	dNa-A[6]	dSr-A[1]
T-O(1)	1.59 (3)	1.67 (3)	1.632 (2)	1.640 (4)	1.676 (2)	1.659 (2)	1.644 (2)
T-O(2)	1.52 (3)	1.75 (3)	1.636 (2)	1.649 (3)	1.663 (1)	1.654 (2)	1.658 (1)
T-2(O(3))	1.61 (2)	1.74 (2)	1.673 (2)	1.676 (3)	1.670 (1)	1.668 (1)	1.677 (1)
mean	1.58	1.73	1.654	1.660	1.670	1.662	1.664
O(1)-T-O(2)	114.0 (6)	113.5 (7)	113.7 (3)	112.5 (6)	107.9 (2)	108.1 (3)	114.5 (2)
O(1)-T-O(3)	111.0 (4)	113.1 (3)	112.0 (2)	112.0 (3)	111.1 (2)	111.7 (2)	112.0 (1)
O(2)-T-O(3)	105.7 (4)	103.4 (4)	104.7 (2)	104.9 (4)	107.5 (2)	107.1 (2)	104.3 (1)
O(3)-T-O(3)	109.0 (6)	109.4 (6)	109.2 (3)	109.9 (5)	111.6 (2)	110.8 (2)	109.2 (2)
T-O(1)-T	151.8 (4)		151.8 (4)	148.4 (8)	128.7 (3)	142.1 (4)	141.4 (3)
T-O(2)-T	165.8 (4)		165.6 (4)	166.7 (7)	177.0 (3)	164.2 (4)	177.7 (3)
T-O(3)-T	141.3 (3)		141.3 (2)	142.5 (5)	152.0 (2)	145.6 (2)	147.0 (2)
Ca(1)-30(3)	2.273 (5)		2.270 (5)	2.328 (8)			
Ca(1)-30(2)	2.892 (4)		2.893 (3)	2.918			
Ca(1)-0*	2.615 (18)		2.613 (19)	na			
Ca(2)-30(3)	na		na	2.272 (7)			
Ca(2)-30(2)	na		na	2.889			
Ca(3)-30(3)	2.317 (17)		2.316 (17)	2.356 (11)			
Ca(3)-30(2)	2.971 (16)		2.974 (16)	2.980			

near-zero coordination is not needed.

Whereas positions Ca(1), Ca(2), and Ca(3) were used in ref 2 to model the electron density on the triad axis near a 6-ring, only two positions Ca(1) and Ca(3) were needed for the present refinement. These positions are close to those for dSr-A[1] and have similar populations with 4.4 (2) Ca atoms displaced into the supercage and 1.2 (2) into the sodalite unit based on the pseudocell. The *electron density* for the combined population of 5.6 Ca atoms is consistent with the electron microprobe analysis of ~5.2 Ca + 0.4 Na plus a possible trace of Mg and K (see earlier), when account is taken of possible errors. It will now be assumed that there is deficiency of exchangeable cations with respect to the electron probe value of 11.5 Al. One possibility is that some of the Al is not in the framework, and indeed the X-ray refinement of 0.3 Al atoms in site Al* could reduce the exchangeable Al to 11.2 Al, which is closer to but still higher than the 10.8 atoms required for simple balance with 5.2 Ca and 0.4 Na in the electron microprobe analysis, but is indistinguishable from the value of 11.2 atoms required to balance the population factors before conversion of some Ca into Na. It is concluded that all data are consistent with a cell content near $Ca_{5.3}Na_{0.4}Al_{11.0}Si_{13.0}O_{48}\cdot(Al_{0.3}O_{0.6}H_{0.3}\cdot xH_2O)$, in which the suggested content of H in the occluded alumina complex is completely speculative.

Conversion of the electron density for site Ca(4) in the refinement by Firor and Seff[2] from Ca to K results in a cell content of five Ca atoms in the 6-rings and one K atom in the 8-rings. The resulting total of 11 charges is identical with the proposed value for the present structure and is consistent with an Al/Si ratio less than unity. The conclusions in ref 7 for the spatial distribution of Ca and Cs atoms for dCa_xCs_{12-2x}-A must be modified if the present evidence is accepted that Ca atoms do not enter the 8-rings. In particular, the curves for Ca^{2+} near 6- and near 8-rings must begin at six and zero atoms, respectively, instead of at five and one for an A crystal with Si/Al equal to unity. Subramanian and Seff argued that their population refinements indicate 12 cation charges (Table II, 11.7 to 12.2) and disputed the arguments by Pluth and Smith[5] for ~11.5 charges. In view of the problems with the refinements in ref 2 and 3, it seems desirable to repeat the study of Ca,Cs-A with crystals that have been chemically analyzed. In particular, a study is needed of the possible development of an AlO_4* complex during ion exchange. In addition, further studies are needed of crystals exchanged with Eu[8,9] and Cd[10] to check the claims of near-zero-coordination for these divalent species.

The new conclusion that all Ca atoms enter only the 6-rings is consistent with the distinct change of absorption as four Na in each pseudocell are replaced by two Ca to yield eight cations,[11] and the explanation in terms of the opening of one out of the three 8-rings per supercage.[12]

For the present structure refinement, both types of Ca atoms are bonded closely to three O(3) at ~2.27 Å and less closely at ~2.89 Å to three O(2) of a 6-ring (Table III). The shorter distances are probably too long because one-quarter of the 6-rings are unoccupied by Ca and are probably less distorted than the occupied ones. The distance of 2.27 Å is at the lower limit of the range of Ca–O distances in aluminosilicates, and is consistent with the small number (three) of first neighbors.

Approximately four-fifths of the Ca atoms project into the supercage (site 1) and one-quarter into the sodalite unit (site 2). A discussion of a possible relation to the deviation of the Si/Al ratio from unity will be presented later.

Aluminum–Oxygen Complex. It is sufficient to state that the new data for dCa-A are fully consistent with the data and interpretation given for dSr-A.[1]

Acknowledgment. This work was supported primarily by National Foundation Grant CHE 80-24138 and secondarily by the Materials Research Laboratory funded by NSF Grant 79-24007. We acknowledge financial support from Union Carbide Corp. given in memory of Donald W. Breck. We thank I. M. Steele, A. M. Davis, N. Weber, O. Draughn, and R. Draus for technical help and G. T. Kokotailo for material assistance.

Supplementary Material Available: A listing (Table IV) of the observed and calculated structure factors (3 pages). Ordering information is given on any current masthead.

(7) Subramaniam, V.; Seff, K. *J. Phys. Chem.* **1980**, *84*, 2928–2933.
(8) Firor, R. L.; Seff, K. *J. Am. Chem. Soc.* **1976**, *98*, 5031–5033.
(9) Firor, R. L.; Seff, K. *J. Am. Chem. Soc.* **1977**, *99*, 1112–1117.
(10) McCusker, L. B.; Seff, K. *J. Am. Chem. Soc.* **1978**, *100*, 5052–5057.
(11) Breck, D. W.; Eversole, W. G.; Milton, R. M.; Reed, T. B.; Thomas, T. L. *J. Am. Chem. Soc.* **1956**, *78*, 5963–5971.
(12) Reed, T. B.; Breck, D. W. *J. Am. Chem. Soc.* **1956**, *78*, 5972–5977.